

Discovery of the Antibiotic Polyketide Tatiomicin via a Genomics Guided Analysis of *Amycolatopsis* sp. DEM30355

Bernhard Kepplinger,^{[a], [f], [h]} Joseph Cowell,^[b] Stephanie Morton-Laing,^[b] Corinne Wills,^[b] Emma C. L. Marrs,^[c] John D. Perry,^[c] Joe Gray,^[d] Michael Goodfellow,^[e] Jeff Errington,^{[f], [h]} Michael R. Probert,^[b] William Clegg,^[b] Jonathan Bogaerts,^[g] Wouter Herrebout,^[g] Nick E. E. Allenby*^[h] and Michael J. Hall*^[b]

[a] Biopharmaceutical Bioprocessing Technology Centre, Newcastle University, Newcastle upon Tyne, NE1 7RU (UK)

[b] Chemistry, School of Environmental and Natural Sciences, Newcastle University, Newcastle upon Tyne, NE1 7RU (UK)

[c] Department of Microbiology, Freeman Hospital, Newcastle upon Tyne, NE7 7DN (UK)

[d] Pinnacle Laboratory, Institute for Cell and Molecular Biosciences, Newcastle University, Newcastle Upon Tyne, NE2 4AX (UK)

[e] Biology, School of Environmental and Natural Sciences, Newcastle University, Newcastle upon Tyne, NE1 7RU (UK)

[f] Centre for Bacterial Cell Biology, Biosciences Institute, Newcastle University, Newcastle Upon Tyne, NE2 4AX (UK)

[g] Department of Chemistry, University of Antwerp, Groenenborgerlaan 171, 2020 Antwerp (Belgium)

[h] Demuris Limited, The Biosphere, Draymans Way, Newcastle Helix, Newcastle upon Tyne, NE4 5BX (UK)

E-mail: michael.hall@newcastle.ac.uk; nick.allenby@demuris.co.uk

Abstract: The application of genomic techniques to the investigation of understudied species of actinobacteria provides an expedited route to the discovery of new bioactive natural products. We report the isolation of the antibiotic polyketide tatiomicin, through a genomics and bioactivity informed analysis of the metabolome of the extremophile *Amycolatopsis* sp. DEM30355. Structural elucidation including absolute stereochemical assignment was performed using complementary crystallographic, spectroscopic and computational methods. Tatiomicin shows antibiotic activity against Gram-positive bacteria, including Methicillin-resistant *Staphylococcus aureus* (MRSA).

Keywords: polyketide • chirality • antibiotic • bacterial natural products • VCD • XRD

The rise of antibiotic-resistant pathogenic bacteria has prompted significant efforts in the development of new small molecule antibiotics,^[1] resulting in a resurgence of interest in natural product research.^[2] Actinobacteria are a rich source of antibiotic natural products, with current developments in this area being fuelled by the application of next-generation whole-genome sequencing technology in combination with advanced bioinformatic analysis.^[3] However, the application of genomic techniques to understudied, extremophilic, unculturable or rare bacterial genera has yet to become widespread, despite the potential for the discovery of molecular novelty that such an approach entails. We therefore decided to investigate the metabolome of the extremophile *Amycolatopsis* sp. DEM30355,^[4] through a combined genomics and bioactivity informed isolation approach resulting in the discovery of a novel anthracenone polyketide we have named tatiomicin. Following structural assignment, absolute stereochemistry was determined through a combination of crystallographic, spectroscopic and computational methods, supporting the recent reassignment of the absolute stereochemistry of its nearest known natural product congeners the rishirilides.^[5] Tatiomicin shows antibiotic activity against a focussed group of Gram-positive bacteria

(including clinically relevant multidrug-resistant *Staphylococcus aureus* (MRSA) isolates). Our preliminary experiments to elucidate the mechanism of action of tatiomicin point towards interference in the RNA synthesis pathway.

Actinomycete DEM30355 was isolated from a soil sample, collected from the El Tatio geyser field within the hyper-arid Atacama Desert region of Chile.^[6] Strain DEM30355 was recovered in the genus *Amycolatopsis*, based on 16S rRNA analysis, forming a subgroup with *A. vancoresmycina* DSM 44592^T and *A. bullii* SF27^T. The genus *Amycolatopsis* contains 76 species and four subspecies encompassing both extremophiles and producers of bioactive secondary metabolites, including the clinically used vancomycin and rifamycin antibiotics,^[7] thus we decided to examine the genome of *Amycolatopsis* sp. DEM30355 for novel biosynthetic potential. Purified genomic DNA from *Amycolatopsis* sp. DEM30355 was analysed using both PacBio[®] and Illumina[®] sequencing technologies and genome assembly was performed using the combined datasets to give a 9.6 Mb draft genome, in 13 contigs. The draft genome of *Amycolatopsis* sp. DEM30355 was examined using the secondary metabolite prediction software AntiSMASH 5.0.0beta1.^[8] Of the 31 biosynthetic gene clusters (BGCs) detected, a type II PKS cluster was identified showing moderate overall similarity (71%) to that which encodes the rishirilides A and B.^[9] The rishirilides A and B are anthracenone polyketides, originally isolated from *Streptomyces rishiriensis* OFR-1056. Rishirilide B has been shown to be a moderately potent inhibitor of α 2-macroglobulin, glutathione S-transferase and asparaginyl-*t*-RNA synthetase, whilst little is known about the biological role of rishirilide A (Figure 1).^[5,10]

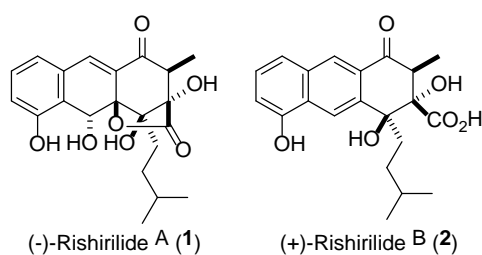


Figure 1. Molecular structures of (–)-rishirilide A (**1**) and (+)-rishirilide B (**2**). Absolute stereochemistry of (+)-**2** and relative stereochemistry of (–)-**1** shown.

Further inspection of the BGC from *Amycolatopsis* sp. DEM30355 revealed a highly altered gene synteny, compared to the rishirilide BGC, along with the presence of several new genes: three postulated to be involved in the PKS biosynthesis (*tatS1*, *tatS2* and *tatS3*), two encoding methyltransferases (*tatM1* and *tatM2*), two encoding cyclases (*tatC4* and *tatC5*). Due to the significant variation in the genetic make-up of the BGC, we postulated that it may code for the production of an as yet undiscovered polyketide and as such we set about attempting to identify this molecule from the metabolome of *Amycolatopsis* sp. DEM30355 (Figure 2).

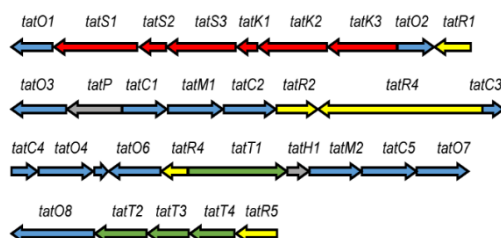
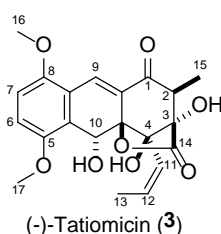


Figure 2. Organization of the tatiomicin BGC. Genes coding for polyketide biosynthesis (red; S = starter unit biosynthesis, K = chain biosynthesis), polyketide modification (blue; O = oxidoreductases, C = cyclases, M = methylases), regulation (yellow), transport (green) and others (grey; P = phosphorylase, H = hypothetical protein).

Preliminary analysis of the fermentation supernatant of the *Actinomyces* sp. DEM30355 by HPLC-HRMS showed the presence of a large number of secondary metabolites, in keeping with the predicted number of BGCs, including a compound with activity against Gram-positive bacteria (MW of 402 Da). Fermentation of *Amycolatopsis* sp. DEM30355, removal of the biomass, extraction of the supernatant and multiple chromatography steps resulted in a fraction which retained antimicrobial activity and contained two closely related compounds. HRMS analysis suggested that these two compounds were stereoisomers of each other, the major compound showing $m/z = 425.1221$ $[M+Na]^+$ corresponding to a molecular formula of $C_{21}H_{22}O_8$. Complete structural assignment of the major component via NMR and single crystal X-ray diffraction (XRD) analysis revealed a highly oxygenated anthracenone polyketide structurally consistent with the BGC of interest, which we named (–)-tatiomicin (**3**).^[11] NMR and HPLC experiments demonstrated that the minor compound was the C-2 epimer, capable of equilibrating with (–)-(**3**) under acidic conditions and as such most likely an isolation artefact (Table 1).

Table 1. Structure and NMR data for (–)-tatiomicin (**3**). Absolute stereochemistry as shown by both vibrational circular dichroism (VCD) and X-ray diffraction (XRD) resonant scattering experiments.



Position	δ_H (J in Hz)	δ_C	Position	δ_H (J in Hz)	δ_C
1	-	196.3, C	9a	-	129.0, C
2	2.78 q (7.6)	49.8, CH	10	5.49 s	66.5, CH
3	-	81.7, C	10a	-	118.9, C
4	-	82.7, C	11	5.47 dq (12.0, 2.0)	124.7, CH
4a	-	83.5, C	12	5.77 dq (12.0, 7.2)	133.2, CH
5	-	151.2, C	13	1.94 dd (7.2, 2.0)	15.6, CH ₃
6	6.92 d, (9.2)	112.8, CH	14	-	174.9, C
7	7.05 d (9.2)	115.9, CH	15	1.20 d (7.6)	11.3, CH ₃
8	-	152.9, C	16	3.84 s	56.4, CH ₃
8a	-	123.3, C	17	3.85, s	56.5, CH ₃
9	8.12 s	131.9, CH	-	-	-

[a] NMR spectra recorded in CD₂Cl₂.

Determination of the absolute stereochemistry of (–)-**3** was undertaken in parallel via circular dichroism spectroscopy and X-ray diffraction (XRD) experiments exploiting resonant scattering. Absolute configuration determination by vibrational circular dichroism (VCD) was based on a comparison of experimental and computationally predicted spectra, taking into account the presence of two epimers of (–)-**3**. Conformational analysis, removal of redundant geometries and final optimization at the B3LYP/6-311++G(d,p) level allowed Boltzmann-weighted VCD spectra for both epimers of (–)-**3** to be constructed. The final predicted spectrum was obtained by applying a 3:1 ratio to account for the experimental mixture analyzed. Numerical analysis was used to establish agreement between experiment and theory, the neighborhood similarity values ($\Sigma^{IR} = 92.0$, $\Sigma^{VCD} = 71.2$, $ESI = -57.8$) suggesting an absolute stereochemical assignment of (2*S*,3*S*,4*R*,4*aR*,10*R*) (Figure 3).^[12] The assignment was supported through similar electronic circular dichroism (ECD) experiments; however, in this case correlation between experiment and prediction was weaker.

To validate the absolute assignment a resonant scattering single-crystal X-ray diffraction experiment, employing synchrotron radiation ($\lambda = 1.4879 \text{ \AA}$ to enhance resonant scattering contributions) was undertaken. The absolute-structure ('Flack') parameter (0.05(6)) was insignificantly different from zero and with a small standard uncertainty, indicating the correct absolute configuration in the refined (2*S*,3*S*,4*R*,4*aR*,10*R*) structure (see SI).^[11] Interestingly, following much stereochemical debate and several reported total syntheses, the absolute stereochemistry of the congeneric (+)-rishirilide B (**2**) was recently revised to (2*S*,3*S*,4*S*), matching that of (–)-(**3**) over the three common stereocenters.^[13]

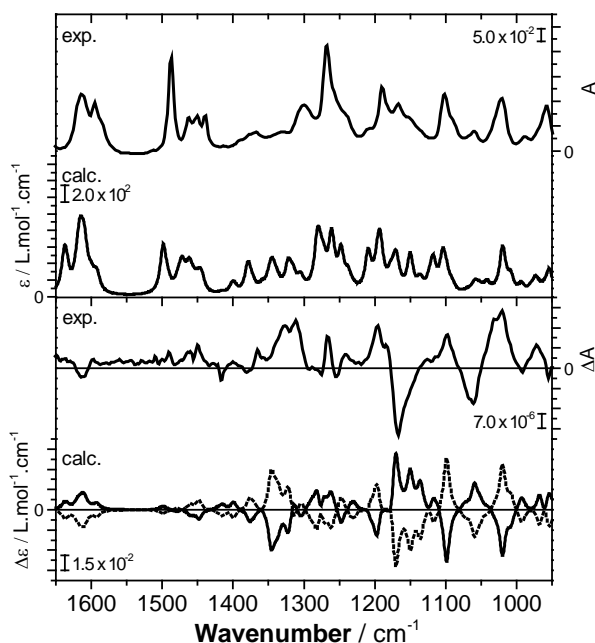


Figure 3. Experimental IR (top) and VCD spectra (bottom) of (–)-tatiomicin **3** (CDCl₃) with predicted spectra obtained at the B3LYP/PCM/6-311++G(d,p) level of theory. VCD: Solid line = (2*R*,3*R*,4*S*,4*aS*,10*S*), dashed line = (2*S*,3*S*,4*R*,4*aR*,10*R*). Spectra have been frequency scaled ($\sigma = 0.987$) to yield maximal similarity between the computed and experimental VCD spectra.

Purified (–)-tatiomicin (**3**) showed no detectable antimicrobial activity (MIC > 64 $\mu\text{g/mL}$) against ten Gram-negative bacteria and two eukaryotic microorganisms (*Candida* sp.) (see SI). However, antibacterial activity was observed against a sub-set of Gram-positive bacteria (MIC = 4–8 $\mu\text{g/mL}$), namely *Staphylococcus* and *Streptococcus* species. Due to the current interest in developing new antibiotics against drug-resistant *Staphylococcus* infections, we further evaluated (–)-**3** against a panel of multidrug-resistant *S. aureus* (MRSA) clinical isolates, including twenty-four EMRSA-15 and EMRSA-16 strains (the main causative agents of nosocomial epidemic MRSA bacteraemia in the UK, with resistance to penicillin, ciprofloxacin and erythromycin),^[14] and twelve MRSA strains isolated from Belgian, Finnish, French and German hospitals. In all cases antibiotic activity was maintained (MIC = 4–8 $\mu\text{g/mL}$), suggesting that (–)-**3** does not operate via a mode of action previously encountered by these strains, prompting us towards further investigation.

Elucidation of the mode of action (MOA) for a new antibacterial agent remains challenging. Characterization of resistance mutations can be informative with respect to the MOA of a molecule, but so far attempts to isolate *Bacillus subtilis* mutants resistant to (–)-tatiomicin (**3**) have been unsuccessful (see SI). Also, no positive responses were seen with a panel of *B. subtilis* strains containing *lacZ* reporter genes used to indicate common antibacterial mechanisms of action, including: fatty acid synthesis (*fabHA*), DNA damage ($\phi 105$ prophage induction), RNA polymerase

(RNAP) inhibition (*helD*), cell wall damage (*ypuA*), gyrase inhibition (*gyrA*), cell envelope stress (*liaI*) (see SI).^[15]

We next undertook a bacterial cytological profiling experiment in which antibacterial induced changes in the morphology of a test bacterium are compared to the those induced by known mode-of-action antibacterials.^[16] *B. subtilis* 168CA-CRW419 expresses two fusion proteins, HbsU-GFP and WALP23-mCherry, allowing simultaneous visualization of both the chromosomal DNA and the bacterial cell membrane by fluorescence microscopy. Interestingly, treatment with (–)-tatiomicin (**3**) induced chromosome decondensation in *B. subtilis* 168CA-CRW419. A similar effect was elicited by the RNAP inhibitor rifampicin. However, further work will be required to establish whether the major effects of (–)-tatiomicin (**3**) are targeted in the RNAP pathway.

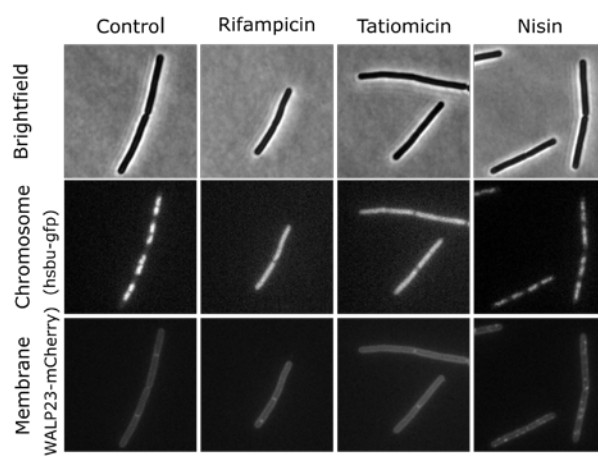


Fig. 5. Single-cell analysis of chromosome and membrane integrity. Phase contrast (top panels) and fluorescence microscopy of *B. subtilis* cells treated with various antibiotics (indicated above). DNA was visualized with an HsbU-GFP fusion (middle panels) and the cytoplasmic membrane with a WALP23-mCherry fusion (bottom panels).

In conclusion, we have demonstrated that the application of a genomics informed, bioactivity guided fractionation approach to rare extremophilic actinobacteria can result in the discovery of new natural products with important bioactivity. Comprehensive structural elucidation of the highly oxygenated anthracenone polyketide (–)-tatiomicin (**3**) included absolute stereochemical assignment by complementary methods (VCD and XRD) providing supporting evidence for the absolute stereochemistry of the related rishirilides. (–)-Tatiomicin (**3**) itself shows promising antibacterial activity against clinically relevant MRSA strains, whilst preliminary experiments indicate a possible molecular target within the RNA transcription pathway.

Acknowledgements

The authors thank Newcastle University (NCL) for funding and PhD scholarships (S.M. & J.C.), EPSRC (EP/G037620/1) for an EngD studentship (B.K.), the Wellcome Trust (B.K. & J.E.) for an Investigator Grant (209500), the Technology Strategy Board (N.E.E.A.) (100953, 131143), the Centre for Process Innovation (CPI) for fermentation and processing support, Diamond Light Source for access to beamline I19 (allocations MT6749 and MT11145), I19 beamline staff for assistance with long-wavelength X-ray experiments, Prof. W. McFarlane (NCL) for NMR support, J. Devi (Demuris) for SEM microscopy and C. Willis (NCL) for the construction of *B. subtilis* strain CRW419.

References

- [1] a) M. A. Fischbach, C. T. Walsh, *Science* **2009**, *325*, 1089-1093; b) H. W. Boucher, G. H. Talbot, J. S. Bradley, J. E. Edwards, D. Gilbert, L. B. Rice, M. Scheld, B. Spellberg, J. Bartlett, *Clin. Infect. Dis.*, **2009**, *48*, 1-12; c) L. L. Silver, *Clin. Microbiol. Rev.* **2011**, *24*, 71-109.
- [2] a) M. S. Butler, M. A. T. Blaskovich, M. A. Cooper, *J. Antibiot.* **2017**, *70*, 3-24; b) A. L. Harvey, R. Edrada-Ebel, R. J. Quinn, *Nat. Rev. Drug Discov.* **2015**, *14*, 111-129; c) M. G. Moloney, *Trends Pharmacol. Sci.* **2016**, *37*, 689-701; d) G. D. Wright, *Nat. Prod. Rep.* **2017**, *34*, 694-701.
- [3] a) J. R. Doroghazi, J. C. Albright, A. W. Goering, K.-S. Ju, R. R. Haines, K. A. Tchalukov, D. P. Labeda, N. L. Kelleher, W. W. Metcalf, *Nat. Chem. Biol.* **2014**, *10*, 963-968; b) A. Milshteyn, J. S. Schneider, S. F. Brady, *Chem. Biol.* **2014**, *21*, 1211-1223; c) N. Ziemert, M. Alanjary, T. Weber, *Nat. Prod. Rep.* **2016**, *33*, 988-1005; d) E. J. Culp, N. Waglechner, W. Wang, A. A. Fiebig-Comyn, Y.-P. Hsu, K. Koteva, D. Sychantha, B. K. Coombes, M. S. Van Nieuwenhze, Y. V. Brun, G. D. Wright, *Nature*, **2020**, *578*, 582-587.
- [4] a) B. Kepplinger, S. Morton, K. Seistrup, E. Marrs, A. Hopkins, J. Perry, H. Strahl, M. J. Hall, J. Errington, N. Allenby, *ACS Chem. Bio.* **2018**, *13*, 207-214; b) H. Mosaei, V. Molodtsov, B. Kepplinger, J. Harbottle, C. W. Moon, R. E. Jeeves, L. Ceccaroni, Y. Shin, S. Morton-Laing, E. C. L. Marrs, C. Wills, W. Clegg, Y. Yuzenkova, J. D. Perry, J. Bacon, J. Errington, N. E. E. Allenby, M. J. Hall, K. S. Murakami, N. Zenkin, *Mol. Cell* **2018**, *72*, 263-274.
- [5] H. Iwaki, Y. Nakayama, M. Takahashi, S. Uetsuki, M. Kido, Y. Fukuyama, *J. Antibiot.* **1984**, *37*, 1091-1093.
- [6] C. K. Okoro, R. Brown, A. L. Jones, B. A. Andrews, J. A. Asenjo, M. Goodfellow, A. T. Bull, *Antonie van Leeuwenhoek* **2009**, *95*, 121-133.
- [7] a) S. Chen, Q. Wu, Q. Shen, H. Wang, *ChemBioChem*, **2016**, *17*, 119-128; b) V. Sangal, M. Goodfellow, J. Blom, G. Y. A. Tan, H.-P. Klenk, I. C. Sutcliffe, *Front. Microbiol.* **2018**, *9*, 2281.
- [8] K. Blin, T. Wolf, M. G. Chevrette, X. Lu, C. J. Schwalen, S. A. Kautsar, H. G. Suarez Duran, E. L. C. de los Santos, H. U. Kim, M. Nave, J. S. Dickschat, D. A. Mitchell, E. Shelest, R. Breitling, E. Takano, S. Y. Lee, T. Weber, M. H. Medema, *Nucleic Acids Res.*, **2017**, *45*, W36-W41.
- [9] a) X. Yan, K. Probst, A. Linnenbrink, M. Arnold, T. Paululat, A. Zeeck, A. Bechthold, *ChemBioChem* **2012**, *13*, 224-230; b) P. Schwarzer, J. Wunsch-Palasis, A. Bechthold, T. Paululat *Antibiotics* **2018**, *7*, 20; c) O. Tsypik, R. Makitrynsky, B. Frensch, D. L. Zechel, T. Paululat, R. Teufel, A. Bechthold, *J. Am. Chem. Soc.* **2020**, *142*, 5913-5917; d) P. Schwarzer, O. Tsypik, C. Zuo, A. Alali, J. Wunsch-Palasis, T. Heitzler, J. Derochefort, M. Bernhardt, X. Yan, T. Paululat, A. Bechthold, *Molecules* **2020**, *25*, 1955.
- [10] a) D. Komagata, R. Sawa, N. Kinoshita, C. Imada, T. Sawa, H. Naganawa, M. Hamada, Y. Okami, T. Takeuchi, *J. Antibiot.* **1992**, *45*, 1681-1683; b) S. C. K. Sukuru, T. Crepin, Y. Milev, L. C. Marsh, J. B. Hill, R. J. Anderson, J. C. Morris, A. Rohatgi, G. O'Mahony, M. Grøtli, F. Danel, M. G. P. Page, M. Härtlein, S. Cusack, M. A. Kron, L. A. Kuhn, *J. Comput. Aided Mol. Des.* **2006**, *20*, 159-178.
- [11] CCDC1584974 and 1584975 contain the supplementary crystallographic data for this paper. These data can be obtained free of charge from The Cambridge Crystallographic Data Centre.
- [12] E. Debie, E. De Gussem, R. K. Dukor, W. Herrebout, L. A. Nafie, P. Bultinck, *ChemPhysChem* **2011**, *12*, 1542-1549.

- [13] a) F. M. Hauser, Y.J.Xu, *Org. Lett.* **1999**, *1*,335-336; b) J. G. Allen, S. J. Danishefsky, *J. Am. Chem. Soc.* **2001**, *123*,351-352; c) K. Yamamoto, M. F. Hentemann, J. G. Allen, S. J. Danishefsky, *Chem. Eur.J.* **2003**, *9*, 3242-3252; d) L. H. Mejorado, T. R. Pettus, *J. Am. Chem. Soc.* **2006**, *128*, 15625-15631; e) M. Odagi, K. Furukori, K. Takayama, K. Noguchi, K. Nagasawa, *Angew. Chem. Int. Ed.* **2017**, *56*, 6609-6612.
- [14] P. C. L. Moore, J. A. Lindsay, *J. Med. Microbiol.* **2002**, *51*, 516-521.
- [15] a) T. Mascher, S. L Zimmer, T. A. Smith, J. D. Helmann, *Antimicrob Agents Chemother.* **2004**, *48*, 2888-2896; b) H. P. Fischer, N. A. Brunner, B. Wieland, J. Paquette, L. Macko, K. Ziegelbauer, C. Freiberg, *Genome Res.* **2004**, *14*, 90-98; c) A. Urban, S. Eckermann, B Fast, S. Metzger, M. Gehling, K. Ziegelbauer, H. Rübsamen-Waigmann, C. Freiberg *Appl Environ Microbiol.* **2007**, *73*, 6436-6443.
- [16] a) P. Nonejuie, M. Burkart, K. Pogliano, J. Pogliano, *Proc. Natl. Acad. Sci. U.S.A.* **2013**, *110*, 16169-16174; b) A. Lamsa, J. Lopez-Garrido, D. Quach, E. P. Riley, J. Pogliano, K. Pogliano, *ACS Chem. Biol.* **2016**, *11*, 2222–2231.